

Monte Carlo simulations of global Compton cooling in inner regions of hot accretion flows

Fu-Guo Xie,^{1,4*} Andrzej Niedźwiecki,^{2*} Andrzej A. Zdziarski^{3*} and Feng Yuan^{1*}

¹Key Laboratory for Research in Galaxies and Cosmology, Shanghai Astronomical Observatory, Chinese Academy of Sciences, 80 Nandan Road, Shanghai 200030, China

²Department of Astrophysics, University of Łódź, Pomorska 149/153, 90-236 Łódź, Poland

³Centrum Astronomiczne im. M. Kopernika, Bartycka 18, 00-716 Warszawa, Poland

⁴Kavli Institute for Astronomy and Astrophysics, Peking University, Beijing 100871, China

1 November 2018

ABSTRACT

Hot accretion flows such as advection-dominated accretion flows are generally optically thin in the radial direction. Thus photons generated at some radii can cool or heat electrons at other radii via Compton scattering. Such global Compton scattering has previously been shown to be important for the dynamics of accretion flows. Here, we extend previous treatments of this problem by using accurate global relativistic Monte Carlo simulations. We focus on an inner region of the accretion flow ($R \leq 600R_g$), for which we obtain a global self-consistent solution. As compared to the initial, not self-consistent solution, the final solution has both the cooling rate and the electron temperature significantly reduced at radii $\gtrsim 10$ gravitational radii. On the other hand, the radiation spectrum of the self-consistent solution has the shape similar to that of the initial iteration, except for the high-energy cut-off being at an energy lower by a factor of ~ 2 and the bolometric luminosity decreased by a factor of ~ 2 . We also compare the global Compton scattering model with local models in spherical and slab geometry. We find that the slab model approximates the global model significantly better than the spherical one. Still, neither local model gives a good approximation to the radial profile of the cooling rate, and the differences can be up to two orders of magnitude. The local slab model underestimates the cooling rate at outer regions whereas it overestimates that rate at inner regions. We compare our modelling results to observed hard-state spectra of black-hole binaries and find an overall good agreement provided any disc outflow is weak. We find that general-relativistic effects in flows which dynamics is modified by global Comptonization is crucial in approaching this agreement.

Key words: accretion, accretion discs – black hole physics – X-rays: binaries – X-rays: general.

1 INTRODUCTION

The lowest-order interaction between photons and electrons, namely Compton scattering, results in momentum and energy exchange. It is a common and important process in astrophysics. The momentum exchange regulates accreting gases to accrete only below a critical value, corresponding to the Eddington limit on the luminosity, L_E (for spherical accretion). The importance of energy exchange manifests itself in two aspects. For photons, Compton up-scattering by energetic electrons is the main mechanism to produce X-ray emission in various astrophysical systems, and Compton down-scattering by low-energy electrons often leads to mod-

ification of X-ray spectra. For electrons, they either gain or lose energy, depending on the average photon energy. This process is important, in particular, in hot accretion flows.

Hot accretion flows such as advection-dominated accretion flows (ADAF, e.g., Narayan & Yi 1994; Abramowicz et al. 1995) are optically thin in both vertical and radial directions. Thus, a photon can travel a long distance before being absorbed or scattered (e.g., Narayan & Yi 1994; Narayan, Mahadevan & Quataert 1998). Then, photons produced in one location can either cool or heat the flow in another location, and Compton effect is not local but *global*. The extension of ADAF to higher accretion rates (but still below the Eddington limit), namely luminous hot accretion flows (LHAF, Yuan 2001 hereafter Y01; Yuan 2003), should be even more affected by the global Compton scattering, since its optical depths are higher and the radiation fields are stronger than those of an ADAF.

* E-mail: fgxie@shao.ac.cn (FGX), niedzwiecki@uni.lodz.pl (AN), aaz@camk.edu.pl (AAZ), fyuan@shao.ac.cn (FY)

Global Compton cooling effects due to external photon sources like the surface of a neutron star have been investigated in the past (e.g., Narayan & Yi 1995). In this study, we concentrate on pure hot accretion flows (ADAF or LHAF) where all the seed photons for Compton scattering processes are generated within the hot plasma. We note that if the geometry of an accretion flow is an inner hot flow plus an outer truncated thin disc (e.g., Esin, McClintock & Narayan 1997), cooling by the outer thin disc (Shakura & Sunyaev 1973) should also be included; however, we neglect it here for simplicity.

While Comptonization in the vertical direction is included in the standard ADAF/LHAF models by a local one-zone treatment (e.g., Narayan & Yi 1995; Manmoto, Mineshige & Kusunose 1997), any non-local radiative transfer in the radial direction, especially Comptonization, has been neglected in almost all of the previous works in this field. Global Comptonization in hot accretion flows has been considered, as far as we know, only by Esin (1997), Kurpiewski & Jaroszyński (1999), Park & Ostriker (1999, 2001, 2007), and recently by Yuan, Xie & Ostriker (2009, hereafter YXO09). We note that only YXO09 and Kurpiewski & Jaroszyński (1999) attempted to find a global solution to this problem rather than to use a self-similar approach, which fails at the inner regions, where most of the radiation is generated. YXO09 used an iteration method to find, for the first time, the radiative cooling rate mutually consistent between the dynamics and radiation of the flow. They have found that Compton heating and cooling dominates outside and inside, respectively, of $\sim 10^4 R_g$, where $R_g = GM_{\text{BH}}/c^2$ is the gravitational radius and M_{BH} is the black-hole mass. They have also found that the relative effect of global Comptonization increases with the increasing accretion rate.

We note, however, that YXO09 have concentrated on the Compton heating of the outer flow. Also, the only photon production rate they used was from the intrinsic emission (synchrotron and bremsstrahlung) and their local Comptonization at a given radius. Thus, although they did calculate the effect of the Compton energy exchange (using the exact relativistic treatment of Guilbert 1986) on the electron temperature in a given radius including photons produced at all radii, they did not take into account the photons generated after the non-local scattering. Thus, non-locally scattered photons were assumed to leave the flow. Since outer parts of hot flows are very optically thin, this is a reasonable assumption for calculating their Compton heating.

On the other hand, here we consider Compton cooling of an inner part of a hot flow, where the Thomson optical depth becomes comparable to unity at moderate accretion rates. Thus, we cannot use the method of YXO09. Instead, we use a Monte Carlo (hereafter MC) method for Comptonization in the hot flow. Our method is directly based on that of Niedźwiecki (2005) and Niedźwiecki & Zdziarski (2006, hereafter NZ06), which is a generalization of the method of Pozdnyakov, Sobol' & Sunyaev (1983) and Górecki & Wilczewski (1984) to include effects of special and general relativity (hereafter GR) and the bulk motion of the flow. Comptonization by bulk motion (considering inflow only) was earlier studied by, e.g., Titarchuk, Mastichiadis & Kylafis (1997) and Laurent & Titarchuk (1999; see also NZ06 for a critical discussion). We assume that electrons have a relativistic Maxwellian distribution, without any non-thermal contribution. In our dynamical treatment, we use a one-dimensional model, which assumes the flow to be both azimuthally and tangentially uniform, with the scale height given by hydrostatic equilibrium.

MC simulations for Compton scattering process in a hot accretion flow in the Kerr metric was first done by Kurpiewski &

Jaroszyński (1999). However, their dynamical model was based on the fully advection-dominated flow (i.e., with negligible radiative cooling), which is clearly not the case for flows with higher accretion rates, which we investigate here.

We describe our treatment of the problem in Section 2. We present a comparison of various Comptonization models in Section 3. In Section 4, we discuss the effects of outflows and viscous electron heating on the accretion solutions. The self-consistent solution for our chosen accretion rate is discussed in Section 5. Our results are compared with observations in Section 6, and conclusions are given in Section 7.

2 THE MODEL

Here, we state the problem we are solving, and present the dynamical equations and the Compton scattering method we use. We focus on a hot accretion flow around a stellar black hole with $M_{\text{BH}} = 10M_{\odot}$. The outer boundary is set at $R_{\text{out}} = 600R_g$ and the accretion rate there is \dot{M}_0 .

In order to study the effect of global Comptonization, we need to know the structure of the flow, i.e., the density, temperature and velocity as functions of the radius. We iterate between the dynamical solutions and the MC Comptonization results to obtain the self-consistent Compton cooling rate. We start from solving the dynamical structure without considering the global Comptonization, which is customary in most of the previous work on hot accretion flows (e.g., Narayan & Yi 1995; Manmoto et al. 1997; Quataert & Narayan 1999; Yuan, Quataert & Narayan 2003). Then we calculate the radially-dependent Compton cooling by the MC simulations. We then use this rate to calculate again the dynamical structure. We repeat the above procedure until it converges.

2.1 Dynamical equations of hot accretion flows

The scale height, H , of the hot accretion flow in our solution depends on the radius. It is given by hydrostatic equilibrium,

$$H = \left(\frac{p}{\rho}\right)^{1/2} \frac{1}{\Omega_K}, \quad (1)$$

where p is the total pressure, which includes contributions from electrons, ions and magnetic field (see below), and ρ is the mass density, where we assume cosmic abundances with the H mass fraction of $X = 0.75$. We assume that the density is tangentially uniform from the disc mid-plane up to $\pm H$. We adopt the pseudo-Newtonian potential of Paczyński & Wiita (1980), in which Ω_K (the Keplerian angular velocity) is given by,

$$\Omega_K = \left[\frac{GM_{\text{BH}}}{R(R - 2R_g)}\right]^{1/2}. \quad (2)$$

Because of the effect of outflow/convection, the mass inflow rate is function of radius and we assume it to be given by

$$\dot{M}_{\text{inflow}} = -4\pi R H \rho v = \dot{M}_0 \left(\frac{R}{R_{\text{out}}}\right)^s, \quad (3)$$

where v (< 0 for the inflow) is the radial velocity. Hereafter, we adopt the unit of $\dot{M}_E = L_E/c^2$ for \dot{M}_0 , where $L_E \equiv 4\pi GM_{\text{BH}} m_p c / \sigma_T$ is the Eddington luminosity for pure H, m_p is the proton mass and σ_T is the Thomson cross section. The value of s is well constrained in the case of the supermassive black hole in our Galactic Centre (Yuan, Quataert & Narayan 2003), and we set $s = 0.3$ follow-

ing that work. We discuss the validity and consequences of this assumption in Sections 4 and 6 below.

The energy equation for electrons is,

$$\rho v \left(\frac{d\varepsilon_e}{dR} - \frac{p_e}{\rho^2} \frac{d\rho}{dR} \right) = \delta q_{\text{vis}} + q_{\text{ie}} - q_{\text{syn+br}} - q_{\text{comp}}, \quad (4)$$

where ε_e is the specific internal energy of electrons, p_e is the electron pressure, and q_{ie} is the electron heating rate per unit volume by ions via Coulomb collisions. The electrons can also be directly heated at the rate δq_{vis} , where q_{vis} is the viscous heating rate per unit volume. We assume $\delta = 0.5$, again following the detailed study of the Galactic Centre accretion flow of Yuan et al. (2003). The electrons are cooled by synchrotron and bremsstrahlung, $q_{\text{syn+br}}$, and by the Compton scattering process, q_{comp} . The latter is the net Compton cooling rate, which is, by definition,

$$q_{\text{comp}} = n_e \int \sigma(E, T_e) \frac{J_E}{E} (\langle E_1 \rangle - E) dE. \quad (5)$$

Here, J_E is the mean intensity per unit photon energy, E , in the local rest frame at R , $\sigma(E, T_e)$ is the Compton cross section averaged over the electron Maxwellian distribution at the temperature, T_e , and $\langle E_1 \rangle$ is the average photon energy (in the same frame) after scattering. However, since we use MC simulations (see Section 2.2) to find our self-consistent solution, we calculate the (equivalent) Compton energy exchange rate directly from the simulations instead of using equation (5). This rate differs from the local Compton cooling rate (commonly used in other studies of hot accretion flows) in that J_E includes now photons either produced or scattered at all radii that reach a given point at R . It can also become negative, i.e., corresponding to the radiative heating by photons, especially in outer regions of the flow ($\gtrsim 10^4 R_g$; e.g., YXO09). However, since we concentrate here on inner flows, we find $q_{\text{comp}} > 0$ in all cases considered here.

We assume the ratio of the gas pressure (electron and ion) to the magnetic pressure, $\beta_B = 9$, i.e., the magnetic pressure of a 1/10th of the total pressure. This parameter determines the strength of the magnetic field in the accretion flow, and the synchrotron emission can then be determined. For it, we follow the method of Narayan & Yi (1995) and Manmoto et al. (1997).

For completeness, we list below the other dynamical equations, i.e., equations for the radial and angular momenta and for the ion energy (see, e.g., Yuan et al. 2003; Manmoto et al. 1997),

$$v \frac{dv}{dR} = -\Omega_K^2 R + \Omega^2 R - \frac{1}{\rho} \frac{dp}{dR}, \quad (6)$$

$$v(\Omega R^2 - j) = -\alpha R p / \rho, \quad (7)$$

$$\rho v \left(\frac{d\varepsilon_i}{dR} - \frac{p_i}{\rho^2} \frac{d\rho}{dR} \right) = (1 - \delta) q_{\text{vis}} - q_{\text{ie}}, \quad (8)$$

where Ω is the angular velocity of the flow, j is the specific angular momentum of the accretion flow when it crosses the horizon, and α is the viscous parameter, which we set here as $\alpha = 0.3$.

We note that except for using the pseudo-Newtonian potential, our dynamical equations are non-relativistic (NR). The radial velocity then un-physically exceeds the speed of light in the vicinity of the black hole. We have tried two kinds of corrections for this. First, in modelling the Galactic Centre, Yuan, Shen & Huang (2006) divide the velocity by factor $0.93 \exp(4.26 R_g / R)$, which comes from fitting to corresponding relativistic results. Second, we note that a first-order dynamical relativistic correction is to replace the NR momentum, mv , by γmv , where γ is the Lorentz factor of the flow. We then approximate the actual velocity using the assumption that the velocities in the NR calculations are the actual ones multi-

plied by factor γ . We have compared these two methods and found no significant differences. Here, we use the latter treatment.

2.2 Monte Carlo method for Compton scattering

The MC method used here is fully GR in the Kerr metric, and it is described in Niedźwiecki (2005) and NZ06. However, in the present paper we consider only a non-rotating black hole. We thus use the following dimensionless parameters,

$$r = \frac{R}{R_g}, \quad \lambda = \frac{Lc}{E_{\text{inf}} R_g}, \quad \lambda_\phi = \frac{L_\phi c}{E_{\text{inf}} R_g}, \quad \beta^r = \frac{v^r}{c}, \quad \beta^\phi \equiv \frac{v^\phi}{c}, \quad (9)$$

where $\mathbf{L} = \mathbf{R} \times \mathbf{p}$ is the vector of the photon angular momentum, $\mathbf{p} = (p_R, p_\theta, p_\phi)$ is the photon momentum vector, $\mathbf{R} = (R, 0, 0)$, L_ϕ is the component of \mathbf{L} parallel to the symmetry axis, i.e., $L_\phi = L \cos \xi$, and ξ is the (dihedral) angle between the plane of photon motion and the equatorial plane. Then, E_{inf} is the photon energy at infinity, v^r and v^ϕ are the radial and azimuthal velocities of the flow, respectively, with respect to local static observers (i.e., observers with r, θ and $\phi = \text{constant}$). We use the relativity-corrected (as described above) values of v and $R\Omega$ as v^r and v^ϕ , respectively.

The tangential motion of the accretion flow is neglected, $v^\theta = 0$. The tangential (or vertical) position of a photon within the flow is given by θ . The energy generation and exchange rates, q , are defined in the rest frame of the flow. Seed photons are randomly generated following the radial distribution of $q_{\text{syn+br}}(r)$ and are assumed to be isotropic in the local rest frame. The flow is assumed to be uniform tangentially, and thus photons are generated uniformly in θ . Then, we follow the photon trajectory in the curved spacetime through subsequent scatterings until the photon either crosses the event horizon or escapes the flow. In the latter case, it then contributes to the observed angle-dependent spectrum.

Note that the optical depth in a relativistic flow around a black hole is affected by both special and general relativistic effects (see NZ06 for a detailed discussion). The following form is valid for electron scattering in the Schwarzschild metric, in a spiral rotating flow with $v^\theta = 0$,

$$d\tau = n_e \sigma(E, T_e) \gamma \times \left\{ 1 \pm \beta^r \left[1 - \frac{\lambda^2}{r^2} \left(1 - \frac{2}{r} \right) \right]^{\frac{1}{2}} - \beta^\phi \frac{\lambda_\phi}{r \sin \theta} \left(1 - \frac{2}{r} \right)^{\frac{1}{2}} \right\} \left(1 - \frac{2}{r} \right)^{-\frac{1}{2}} d\zeta, \quad (10)$$

where ζ is the affine parameter. The upper and lower sign above corresponds to ingoing (i.e. with $dr/d\zeta < 0$) and outgoing photons, respectively (note that $\beta^r < 0$).

The simulation of Compton scattering is performed in the local rest frame using the MC method of Górecki & Wilczewski (1984; see also Pozdnyakov et al. 1983). The electron temperature, the density, and the velocity vector are found in each iteration from the hydrodynamical solution by interpolating between values calculated at 57 logarithmically spaced radii, r_i (such a grid is sufficient given a smooth distribution of the flow parameters).

In order to allow us to compare our results with some previous models, which usually neglect general and special relativistic effects and use local approximations for Comptonization, we perform also calculations for local models. We define a set of 57 uniform, independent spheres or infinite slabs with the n_e , T_e , and the seed spectrum (synchrotron and bremsstrahlung) given for each r_i . The sphere radius or the slab half-thickness are given by the corresponding scale height of the flow, H_i . Then, the Thomson optical depth corresponding to the sphere radius or the slab half depth is $\tau_{T,i} = \sigma_T n_e(r_i) H_i$. We then use the MC Comptonization method

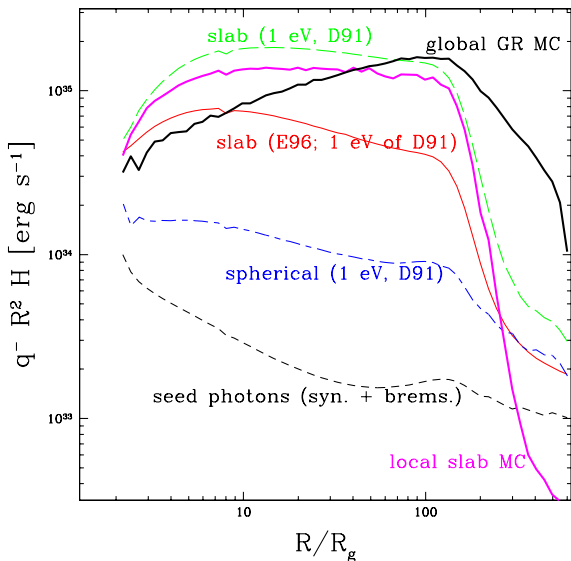


Figure 1. The cooling rates times volume, $q^- R^2 H$, for models based on the dynamical properties of the initial solution with $\dot{M}_0 = 0.5\dot{M}_E$. The black dashed curve gives the rate due to the synchrotron and bremsstrahlung emission. The thick magenta and black solid curves correspond to the local slab model and global GR Compton scattering model, respectively, both of them obtained using the MC method. The thin red solid curve gives the cooling rate using the local slab model of E96 but with the optical depth from D91 for their 1-eV seed photon case. The blue short-long dashes and green dashes correspond to the local approximation with the model of D91 for a sphere and slab, respectively, with the coefficients tabulated for 1-eV seed photons. See Section 3 for details.

in flat space for each slab or sphere. The *local* Compton cooling rate can then be determined for each slab or sphere, while the total luminosity is the sum of the radiation from all the 57 slabs or spheres.

3 COMPARISON OF COMPTONIZATION MODELS OF HOT FLOWS

We first consider some Comptonization models used in other works and compare them with our results. A quantity often used to quantify the effect of thermal Compton up-scattering is the amplification factor, η , by which the power in initial seed photons is amplified through Compton scattering. In our formalism,

$$\eta(r) = \frac{q_{\text{syn+br}}(r) + q_{\text{comp}}(r)}{q_{\text{syn+br}}(r)}. \quad (11)$$

In local models, it is assumed that only photons produced at r are Comptonized at this radius. The amplification factor of the Comptonization depends on the local electron temperature, T_e , the Thomson optical depth, τ_T , and on the initial photon energy, E_i . Here, we use the formalisms of Esin et al. (1996, hereafter E96) and of Dermer, Liang & Canfield (1991, hereafter D91), averaging their E_i -dependent η over our seed spectra to get the corresponding Compton cooling rate. We note whereas E96 give an approximate formula that is supposed to be valid for any E_i , equations (1), (20), and table 1 of D91, which we use here, contain coefficients tabulated at $E_i = 1$ eV and 1 keV only. Thus, their formula is accurate only for those values of E_i in spite of the appearance of E_i as an argument of their equation (1).

Fig. 1 shows the cooling rates for the dynamical solution given by the initial iteration in Section 5 at $\dot{M}_0 = 0.5\dot{M}_E$. In this initial iteration only, local slab Comptonization is applied (in order to get the first iteration of the dynamical solution), and the Comptonization cooling (shown as thin red solid curve) is treated using equation (A10) of E96 and equation (20) of D91, with coefficients taken from the $E_i = 1$ eV slab case. We use here the 1 eV case since most of our synchrotron seed photons are close to this energy. (The results using the original formulae of E96 are very similar to the thin solid curve and thus not shown here.) In addition to Comptonization cooling rates, we also show the cooling rate due to the intrinsic seed emission via synchrotron and bremsstrahlung processes. Then, the ratio of Comptonization cooling rate to the seed one equals to $\eta - 1$. We also show here the analytical models of D91 for sphere and slab, and compare them to our local NR results and the global GR MC results.

The thick black solid curve shows global GR MC results based on the initial dynamical iteration. We can see that the worst model compared to these accurate results is the spherical one (blue short-long dashes). This is because a sphere is a very poor approximation to the geometry of an accretion flow, more similar to a slab. A key factor affecting Comptonization in hot accretion flows is that the optical depth in the radial direction is much larger than that in the vertical direction (which is ≈ 0.7 from horizon to the outer boundary for the initial solution). Only models with a slab geometry can account for this property. The assumption of a spherical geometry, which ignores the large difference in the radial and vertical optical depths, leads to significant underestimation of the probability of scattering, and thus under-prediction of both the magnitude of the Compton cooling rate by about an order of magnitude (see Fig. 1), and the hardness of Comptonization spectrum, see Section 5 below.

As we see in Fig. 1, although the local slab model provides much better approximation to the radial profile of the cooling rate than the spherical model, deviations with respect to the global GR calculations remain highly significant. The local slab approximation, in either version of E96 or D91, has several deficiencies, which we discuss below.

First, the seed photons in the formalism of D91 are assumed to be at either 1 eV or 1 keV. This is obviously not the case in general. Especially when most of the power in seed photons is at high energies, as it is the case for bremsstrahlung, that formula becomes highly inaccurate. Since typical electron temperatures in hot accretion flows are mildly relativistic, scattering is affected by Klein-Nishina effects. Those effects are also not taken into account by E96. Thus the formulae for the amplification factors from those works usually lead to an overestimation of the Compton cooling rate when bremsstrahlung radiation is the main seed photon source. This can be seen in Fig. 1 at $R \gtrsim 200R_g$, where the local analytical results are way above the local slab MC results.

Second, even more importantly, Comptonization is not local. As shown in Fig. 1, Comptonization can increase the cooling rate by up to two orders of magnitude, i.e., the process is very important. In particular, we see that the cooling rate for global Comptonization is much less centrally concentrated than that for the local treatments. The seed photon production rate itself is centrally concentrated; however, those photons travel to outer regions, increasing the cooling rate there. The local slab model neglects this effect.

Third, strong gravity leads to capture of photons generated in the innermost region of the accretion flow, and redshifts escaping photons. This will be further discussed in Section 5 below.

Fourth, Comptonization on the flow bulk motion may, in principle, be important in addition to Comptonization by electron ran-

dom motion. Here, we have both rotation and inflow. The rotation remains slightly sub-Keplerian throughout most of the flow, and the radial velocity, $v \sim -\alpha\Omega_K R$ (e.g., Narayan & Yi 1994) is significantly smaller than the free-fall velocity. Then, both components of velocity become relativistic only in the innermost part, within a few R_g . The bulk plasma motion can affect the spectrum of the observed radiation through the following effects. (i) Collimation of the radiation along the direction of plasma motion, which in a converging flow around a black hole results in the increase of the number of photons captured by the black hole. On the other hand, photons emitted outward have an increased scattering probability due to the inflow. This increases photon trapping in optically-thick flows. Even in optically thin flows, photons after those scatterings are collimated inward, and mostly captured. (ii) The same effect changes the photon energy after scattering, and the change now is due to both the bulk and thermal motions of the electrons. A condition for the bulk motion to be an important source of energy can be written as $(\gamma - 1)m_e c^2 / (3kT_e) \gtrsim 1$ (e.g., Blandford & Payne 1981), which is virtually never satisfied in advection-dominated accretion flows (see Jaroszyński 2001). In our simulations, we have compared the power transferred to photons in the plasma rest frame (i.e., from thermal motion only) and in the local static frame (with a contribution of bulk motion), and have found that the latter is larger by only ~ 10 per cent greater around $10R_g$. Only at $\approx 2.3R_g$ the flow velocity becomes highly relativistic (and thus motion contributes appreciably), but the contribution of this region to the total radiated power is tiny, as seen in Fig. 1. At $\gtrsim 10R_g$, the effect of bulk motion is completely negligible. Overall, we conclude that the bulk motion Comptonization has only a minor effect for hot accretion flows.

4 EFFECT OF OUTFLOWS AND VISCOUS HEATING OF ELECTRONS ON ADAF SOLUTIONS

Taking into account of disc outflows (e.g., Stone, Pringle & Begelman 1999; Blandford & Begelman 1999) and of viscous heating of electrons (e.g., Bisnovatyi-Kogan & Lovelace 1997; Quataert & Gruzinov 1999; Sharma et al. 2007) represent two progresses of the hot accretion theory since its initial formulation. Including of either of these possible effects influences accretion solutions in a major way. Since in this work we investigate how global Comptonization affects those solutions, for completeness and to enable comparison among all of these effects, we also show how outflows and viscous electron heating modify the accretion flow structure.

Fig. 2 shows a comparison between the ADAF model without an outflow, $s = 0$, and with no viscous electron heating, $\delta = 0$, and models with either s or δ or both being > 0 . These solutions are obtained with local Comptonization using the analytic approximation of E96 and D91 used by us (see Section 3). We see first that adding viscous electron heating has a relatively minor effect. It somewhat increases τ_T and T_e and slightly decreases T_i . On the other hand, including outflows leads to a dramatic decrease of τ_T and relatively strong increase and decrease of T_e and T_i , respectively, with the effects being much stronger in inner flow regions. Then, setting both $s = 0.3$, $\delta = 0.5$ results in a superposition of the individual effects.

These effects can be understood as follows. Increasing δ increases and decreases the power supply to electrons and ions, respectively. An increase of s obviously strongly reduces the density and τ_T . This reduces the radiative cooling (roughly $\propto \rho^2$) faster than the viscous heating ($\propto \rho$), which results in an increase of T_e . The corresponding decrease of T_i is due to the reduced compression work caused by the shallower density profile.

5 RESULTS

Fig. 3 presents comparison between the initial (short-dashed curves) and the final self-consistent (solid curves) global GR MC solutions at $\dot{M}_0 = 0.5\dot{M}_E$. Fig. 3(a) shows the electron and ion, T_i , temperatures. We see that compared to the initial solution, T_e decreases significantly at $\gtrsim 10R_g$, up to a factor of ~ 2 at $(100-200)R_g$. This is an effect of the increased cooling in that region, as we see in Fig. 3(c). On the other hand, there is almost no change in T_i .

The height-to-radius ratio is shown in Fig. 3(b). We find that the height of the flow is nearly unchanged at $\lesssim 20R_g$, and slightly decreases at larger R , which is due to a decrease of T_i (and T_e) there. We also find only relatively small changes in v and n_e . The vertical Thomson optical depth shown in the inset of this panel increases slightly, while it remains nearly unchanged at $\lesssim 10R_g$. The horizontal optical depth of the final solution is 0.75.

Fig. 3(c) compares the cooling rates for the global GR model and also for the local slab model. The final solutions differ significantly from the initial ones. Also, the global MC solutions differ very strongly from those for the local slab model. The final self-consistent profile is relatively flat, namely, drops by only a factor of a few from the maximum at $\sim 10R_g$ to $200R_g$. The flat profile is partly due to the global Compton scattering. Also, there is a very strong outflow in our model, see equation (3). This strongly reduces both \dot{M} and the cooling rate towards the black hole.

Fig. 3(d) shows the spectra of the initial and final solutions from MC simulations with both the local slab and global GR models. We find that the shape of the spectrum remains very similar for the initial and final solutions, but the normalization of the spectra of the final solutions is about a half of that of the initial solution. This is roughly consistent with the result of YX09. The bolometric luminosity of the final model is $L \simeq 8.4 \times 10^{36}$ erg s^{-1} , which is $6.7 \times 10^{-3} L_E$. If we define the radiative efficiency as $L / (\dot{M}_0 c^2)$, it will be 0.013. However, we stress that most of the potential energy of the flow at R_{out} is lost to the assumed outflow.

For either the initial or final solution, the spectral differences between the global GR and local slab models are relatively small, in particular much smaller than the differences in the cooling rate. This is because each spectrum is the sum of the radiation produced at all radii, which averages the local differences. For the final self-consistent solution, the difference between the global and local models is significant mostly at the high energy end, $\gtrsim 100$ keV. This is because this part of the spectrum is produced by Comptonization in the innermost part of the flow, where the capture by the black hole and other GR effects are strong, which reduces the energy of the high-energy cut-off. A corresponding difference for the initial solutions does not appear because the high-energy radiation does not originate from the innermost region, as we can see in Fig. 3(c). The differences in the soft X-ray/UV bands are also caused by the capture and redshift effects. We also see that the local spherical MC model leads to a strong under-prediction of the hardness of the spectrum, see the dotted curve in Fig. 3(d).

When the accretion rate increases (but still $L \ll L_E$), the radiative cooling will exceed the local viscous heating, and the accretion flow will enter into the LHAF regime (Y01). The accretion flow can still remain hot because of the heating by the compression work (Y01) and it is the sum of the viscous dissipation and the compression work that balances the radiative cooling. Above a certain \dot{M}_{crit} , the radiative cooling becomes so strong that the flow cannot remain entirely hot. Such a flow below a certain R (see, e.g., the long dashes in fig. 1 of Y01) will either collapse into a thin disc or switch into a two-phase flow, with cold clumps embedded in the hot phase (Y01,

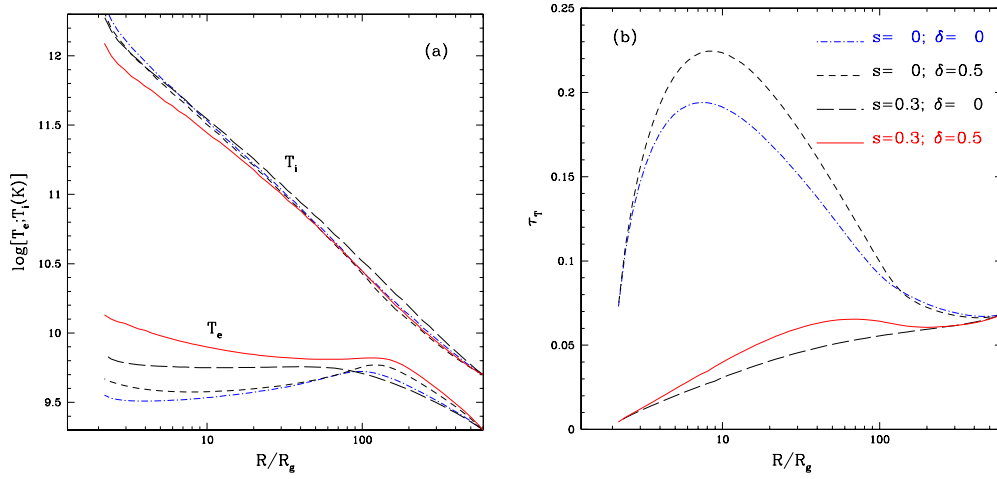


Figure 2. The effect of an outflow (measured by s) and viscous heating of electrons (at the fractional rate of δ) on the ADAF solutions. The dot-dashes, short dashes, long dashes and solid curves show the original ADAF model ($s = \delta = 0$), and models with strong viscous electron heating and no outflow ($s = 0, \delta = 0.5$), with no viscous electron heating but strong outflow ($s = 0.3, \delta = 0$), with both phenomena included ($s = 0.3, \delta = 0.5$). In all models, Comptonization is treated analytically (D91; E96), and $\dot{M}_0 = 0.5\dot{M}_E$. (a) The radial profiles of the electron (lower curves) and ion (upper curves) temperature. (b) The radial profile of the vertical optical depth.

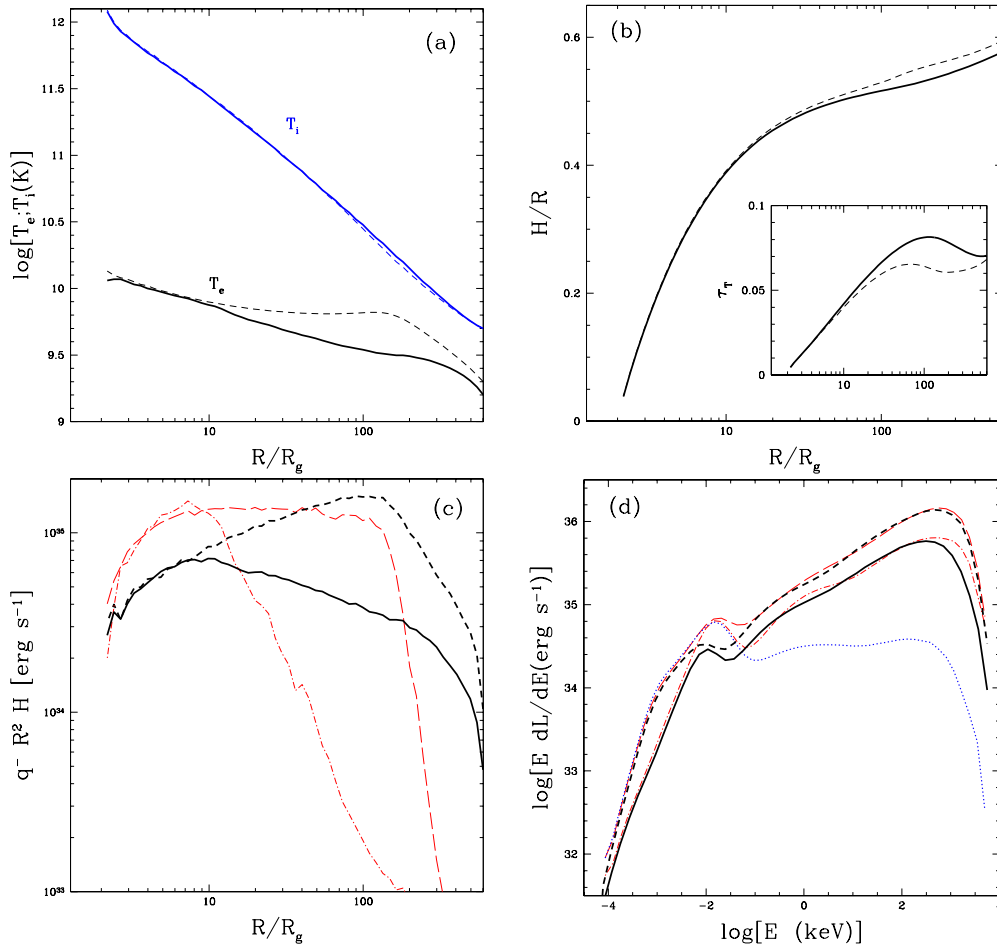


Figure 3. Comparison between the initial (short dashes) and final self-consistent (solid curves) MC solutions with $\dot{M}_0 = 0.5\dot{M}_E$. (a) The radial profiles of the electron (lower curves) and ion (upper curves) temperatures. (b) The ratio of the scale height to the radius, and the vertical optical depth shown in the inset. (c) The radiative cooling rate. (d) The spectrum. In (c–d), the (red) long dashed and dot-dashed curves correspond to local-slab MC simulations of the initial and final solutions, respectively. The blue dotted curve in (d) shows the spectrum from the local-sphere MC simulations for the dynamical structure of the initial solution. [Note that the short and long dashes in (c) are, respectively, the same as the thick solid black and magenta curves in Fig. 1.]

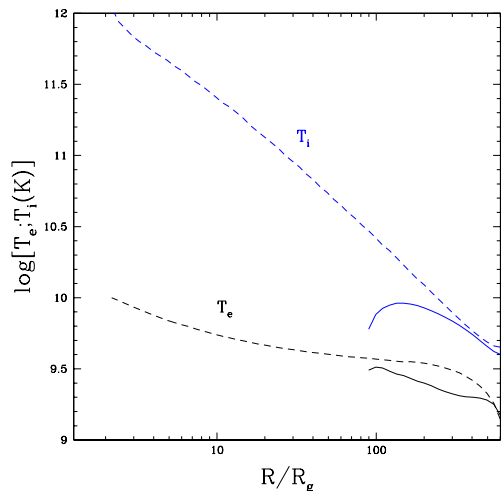


Figure 4. Comparison between the radial profiles of the electron (lower curves) and ion (upper curves) temperatures for MC calculations for the initial (dashed curves) and a solution including global Comptonization (solid curves) for $\dot{M}_0 = 1.0\dot{M}_E$. We see there is no self-consistent solution for $R \lesssim 10^2 R_g$ due to the very strong cooling. At lower radii, either the disc collapses or a two-phase cold/hot flow forms.

Yuan 2003). The value of \dot{M}_{crit} decreases when the global Compton scattering effect is included. Here, we find that at $\dot{M}_0 = 1.0\dot{M}_E$, the flow collapses at $\lesssim 100R_g$, as shown in Fig. 4. Thus, the critical accretion rate for our assumed flow with the strong outflow at $s = 0.3$ is given by $0.5 < \dot{M}_{\text{crit}}/\dot{M}_E < 1.0$. This \dot{M}_{crit} will decrease even further if the cooling due to the photons from outer thin disc is included. We also find that \dot{M}_{crit} is higher in the local-Compton model with the cooling rate of E96 and D91 (as used by us above), $\approx 1.5\dot{M}_E$ (which solution is not presented here) than in the global-Compton model. This value is then lower than that found by Y01, which is in the range of $\sim (3-5)\dot{M}_E$. (Note that Y01 used the definition of \dot{M}_E including an efficiency factor of 0.1.) The discrepancy is because both the strong outflow, which suppresses the compression work (crucial for LHAF), and the strong direct electron heating ($\delta = 0.5$) are included in the present model while they are not in Y01.

6 COMPARISON WITH OBSERVATIONS

Data on the spectral hard state of black-hole binaries show the high-energy cut-off around ~ 100 keV (e.g., Grove et al. 1998; Wardziński et al. 2002; Zdziarski & Gierliński 2004; Done, Gierliński & Kubota 2007; Joinet, Kalemci & Senziani 2008). When this cut-off is parameterized by the maximum in the EdL/dE plots, it is in the range of $\sim 50-200$ keV (for spectra with the photon index < 2 , which is the case in the hard state).

We compare these results with our model spectrum, see Fig. 3(d). The maximum in the EdL/dE spectrum of the initial, not self-consistent, solution is at ≈ 700 keV if GR effects are neglected and Comptonization is local (the long-dashed curve), which then moves to ≈ 600 keV when GR effects are taken into account (the short-dashed curve). The peak energy is at ≈ 500 keV for the self-consistent solution when both global Comptonization and GR effects are neglected (the dot-dashed curve). The value of this peak energy is then very similar to the value of the electron temperature, $kT_e \sim 700$ keV (Fig. 3a) at the radius of the peak dissipation of the corresponding model (Fig. 3c). The final dynamic solution has the

dissipation rate much more centrally concentrated than the initial one, see Fig. 3(c), and then the GR effects reduce the peak energy much more, to ≈ 300 keV (the solid curve). Thus, taking into account Comptonization self-consistently, i.e., as the global process in the entire hot disc, and including the GR effects reduces the peak energy of the spectrum by a factor of $\approx 2/3$. This is because the global Comptonization increases the spectral contribution of outer flow regions while the GR effects reduce the contribution of inner regions. The GR effects here include three parts (see discussion in Section 3), namely the gravitational and Doppler redshift, and the preferential capture of most energetic photons (enhanced by the kinematic collimation) by the black hole. The last effect is the dominant one.

However, this decrease is still not sufficient to bring the theoretical cut-off down to the observed values. This problem appears to be shared by the hot accretion flow model in general, see, e.g., Yuan & Zdziarski (2004). As stated above, the cut-off energy before correcting for the GR effects approximately equals the temperature of the flow in the region where most of the radiation is emitted. Emission of this region can then be roughly approximated as that of a one-zone thermal-Comptonization model. Fits of this model to hard-state spectra of black-hole binaries and of Seyfert galaxies show $kT_e \approx 50-100$ keV, see, e.g., the compilation in Yuan & Zdziarski (2004). Approximately, kT_e of the one-zone model equals the energy of the maximum of its EdL/dE spectrum. The other parameter of this model is the Thomson optical depth, τ_T . For a given X-ray spectral index, the Compton parameter, $y = 4T_e\tau_T$, is approximately constant. Also, kT_e is anticorrelated with τ_T for a given local dissipation rate in a hot flow, reflecting the varying power per electron. Fits of the one-zone thermal-Compton model yield $\tau_T \sim 1$ (e.g., Yuan & Zdziarski 2004) whereas the vertical optical depths of the flow are $\tau_T \ll 1$, see Fig. 3(b), which expresses the same discrepancy as T_e of the flow being too high. As stated above, taking into account the GR effects in the global-Compton model improves the agreement significantly (pointing to the inadequacy of Comptonization models neglecting GR), but not sufficiently.

On the face of it, this discrepancy might indicate that the hot flow model is not applicable to the hard state of black hole binaries and Seyfert galaxies. However, we note that the present calculations assume a very strong outflow, equation (3) with $s = 0.3$, motivated by the modelling of the Galactic Centre (Yuan et al. 2003). On the other hand, our assumed dimensionless accretion rate is \gg that of the Galactic Centre source, whereas the relative strength of outflows appears to decrease with the increasing accretion rate (Gallo, Fender & Pooley 2003; Fender, Belloni & Gallo 2004), as also indicated by a relatively small change of the X-ray bolometric luminosity during hard/soft state transitions (e.g., Zdziarski et al. 2004). This is plausible from a theoretical point of view because the Bernoulli parameter becomes smaller with the increasing accretion rates (Yuan, Cui & Narayan 2005; Bu & Yuan in preparation). Thus, it is likely that the fractional strength of the outflow, 82 per cent for our assumed s , R_{out} and \dot{M}_0 (with 18 per cent of \dot{M}_0 crossing the horizon), may in reality be much weaker. Setting $s = 0$ leads to τ_T being a few times higher and T_e about a factor of two lower, see Fig. 2. Although the calculations in Fig. 2 are done with the local analytical treatment of Comptonization, and are thus not self-consistent, they correctly predict the direction of the changes of the flow parameter. If the characteristic T_e of the self-consistent flow were reduced by the same factor of two with respect to the model with $s = 0.3$, the peak of the EdL/dE spectrum would also go down by a similar factor, bringing it to the observed range and resolving the discrepancy with the data.

Our second assumption has been of a strong viscous heating of electrons, $\delta = 0.5$. As seen in Fig. 2, this has a relatively minor effect on T_e and τ_T . We also note that the half-depth Thomson optical depth of a slab is the quantity closest to that of the half-depth of the flow, and should preferably be used when comparing accretion flow models with one-zone thermal Comptonization models. For a given X-ray spectral index, the optical depth is somewhat lower for a slab geometry than for spherical one.

We note that there is a number of additional effects that can further reduce T_e and increase τ_T , possibly allowing the hot flow model to be in agreement with the full range of the observed hard-state spectra. First, an increase of the black-hole spin reduces the radial velocity and increases the density of the flow. The effect is rather strong, as can be seen, e.g., in fig. 5 of Gammie & Popham (1998). Global Comptonization in the Kerr metric will be studied in detail in our forthcoming work. Second, the presence of moderate large-scale toroidal magnetic fields in the accretion flow significantly reduces T_e , as shown by Bu, Yuan & Xie (2009). Third, electron cooling will also be significantly enhanced in either a two-phase flow, with cold clouds mixed with the hot flow, or, fourth, at presence of an inner collapsed disc, with both effects happening above some critical accretion rate (Section 5, see also Y01, Yuan 2003).

Furthermore, the cut-off energy in the hard state of black-hole binaries is observed to decrease with the increasing luminosity (Wardziński et al. 2002; Yamaoka et al. 2006; Yuan et al. 2007; Miyakawa et al. 2008)¹. Also, the hot-flow characteristic temperature goes down with the increasing accretion rate, in agreement with the observations. In our case, the bolometric luminosity is only $0.007L_E$ (Section 5), and thus our model spectrum should be compared with the hard state at the correspondingly low L (which is somewhat below, e.g., the hard-state range of L of Cyg X-1 of $\approx 0.01\text{--}0.02L_E$, Zdziarski et al. 2002), which spectra are likely to have the cut-off energies > 100 keV. This would be in agreement with our results, after the correction for the outflow discussed above.

Malzac & Belmont (2009) have also pointed out that the ion temperatures implied by observations of the hard state are much lower than those typical for ADAF models. However, the ratio of T_i/T_e , calculated by Malzac & Belmont (2009) directly from the formula for Coulomb energy transfer from ions to electrons, is approximately $\propto \tau_T^{-2}$, and the discrepancy pointed out by those authors occurs at $\tau_T \sim 1$. If we take instead the low values of τ_T obtained in ADAF models, there is an agreement between their estimate and the hot flow models.

On the other hand, we stress that using equation (3) with $s = 0.3$ does not weaken our conclusions related to the role of global Comptonization. Instead, if the outflow is weaker for a given \dot{M}_0 , the radiation generated at small radii and subsequently received at large radii will be stronger, thus the global Comptonization effect will become even more important than for our chosen assumption. This would further reduce the average photon energy of the emitted spectrum.

Another related issue is our determination of the value of the critical accretion rate, at which an inner part of the hot flow collapses. We find it corresponds to a relatively low $L \approx 0.01L_E$. Lu-

minosities of the hard state of black-hole binaries are commonly above this L (e.g. Done et al. 2007; Zdziarski et al. 2002). Again, our determination is for the assumed strong outflow, and relaxing this assumption may increase that critical luminosity. On the other hand, the presence of a collapsed geometrically thin disc close to the horizon would explain the finding of relativistically broadened Fe $K\alpha$ line in the hard state of black-hole binaries (e.g., Miller et al. 2006; Miller 2007; but see Done & Diaz Trigo 2009 for a critical view), whose origin would have otherwise been in conflict with the hot accretion flow model of the hard state.

Finally, we note that alternative models for the hard state have been proposed. A very interesting recent model is non-thermal, in which the power supplied to electrons (with the optical depth of $\tau_T \gtrsim 1$) goes into their acceleration into a power-law distribution (Poutanen & Vurm 2009; Malzac & Belmont 2009). Then, synchrotron self-absorption and Coulomb interactions efficiently thermalize the electrons provided any blackbody emission is weak. This radiative one-zone model fits the hard-state data, e.g., of Cyg X-1, very well. An important issue here is the location of the non-thermal plasma. It cannot be a corona as the model constrains any disc blackbody emission irradiating the plasma to be very weak. If it is an inflow, it would require an efficient mechanism of electron acceleration (instead of heating) with a large δ , and a low radial velocity to achieve the required large τ_T . It appears unclear whether such a model is possible dynamically.

7 CONCLUSIONS

Hot accretion flows, both ADAF and LHAF, are optically thin in the radial direction, and thus the global Compton scattering is important. Its effect on the dynamics of the accretion flow has been investigated previously by an analytical approach in YXO9. In this paper we revisit this problem using the more accurate MC simulations, and focusing on the inner region of the flow. We confirm that the global Compton scattering effect is dynamically very important. We obtain the final self-consistent solution using the iteration approach. Our main results, in particular showing the differences between the initial and final iterations, are presented in Fig. 3. The global GR cooling rate of the final self-consistent solution is more centrally concentrated than that of the initial solution, but less centrally concentrated than the local cooling rate of the final solution.

To evaluate the effect of global Compton scattering, we also compare the global GR Compton scattering model with two local models, in the sphere and slab geometries. In these models, only the local scattering is taken into account. For both the initial and final self-consistent solutions, we find that none of the local models can adequately reproduce the global model, although the slab model is significantly better than the spherical one. This is due to the fact that the radial optical depth of the hot flow is much higher than the vertical one.

Specifically, the local slab model underestimates the cooling rate in an outer region, $\gtrsim 200R_g$, by up to two orders of magnitude with respect to the global GR MC results, while it overestimates the cooling rate by up to factor of a few in an inner region, $\lesssim 20R_g$. These differences occur because of the transfer of seed photons between different radii, mostly from small to large radii. We also find that the main dynamical effect in our self-consistent treatment is the global Comptonization, whereas the GR and bulk motion effects are dynamically less important.

We also compare the spectra of the initial and final solutions in both the local and global models. We find that the shape of the

¹ Note that temperatures as low as ~ 20 keV were claimed in the one-zone model fits in Miyakawa et al. (2008). However, they were obtained using the non-relativistic Comptonization model of Sunyaev & Titarchuk (1980), which is not valid for spectra extending above ~ 50 keV.

spectrum of the final self-consistent solution changes only slightly (mostly in the reduced high-energy cut-off) compared to that of the initial solution, but the normalization decreases by a factor of ~ 2 . We also find that the spectral differences between global and local slab models are much less significant than those in the radial profile of the cooling rate. This is due to the averaging of the local spectra over all radii.

We have compared our results to the spectra of the hard state of black-hole binaries, see Section 6. We find an overall rough agreement, though our models have the characteristic electron temperatures and the characteristic Thomson optical depths higher and lower, respectively, than those required by the observational data. However, this discrepancy can, most likely, be resolved if the disc outflow in the luminous hard states is much weaker than that assumed by us. Additional factors that would allow the model be in agreement with the full range of the observed spectra are the spin of the black hole, large-scale magnetic fields, and the presence of an additional electron cooling mechanism, e.g., soft photons from cold clouds embedded in the hot flow, or from an inner collapsed thin disc. We stress that global Comptonization is crucial in bringing the hot accretion flow model to agreement with the data. This is due to the self-consistent model having the dissipation much more centrally concentrated than that of local models, which in turn causes the GR effects to reduce the spectral cut-off energy much more for the former than the latter.

ACKNOWLEDGMENTS

FGX and FY have been supported in part by the Natural Science Foundation of China (grants 10773024, 10821302, 10825314 and 10833002), One-Hundred-Talent Program of Chinese Academy of Sciences, and the National Basic Research Program of China (grant 2009CB824800). AAZ and AN have been supported in part by the Polish MNiSW grants NN203065933, 362/1/N-INTEGRAL/2008/09/0 and N20301132/1518.

REFERENCES

- Abramowicz M. A., Chen X., Kato, S. Lasota J.-P., Regev O., 1995, *ApJ*, 438, L37
- Bisnovatyi-Kogan G. S., Lovelace R. V. E., 1997, *ApJ*, 486, L43
- Blandford R. D., Begelman M. C., 1999, *MNRAS*, 303, L1
- Blandford R. D., Payne D. G., 1981, *MNRAS*, 194, 1033
- Bu D.-F., Yuan F., Xie F.-G., 2009, *MNRAS*, 392, 325
- Dermer C. D., Liang E. P. Canfield E., 1991, *ApJ*, 369, 410 (D91)
- Done C., Diaz Trigo M., 2009, *MNRAS*, submitted, arXiv:0911.3243
- Done C., Gierliński M., Kubota A., 2007, *A&ARv*, 15, 1
- Esin A., 1997, *ApJ*, 482, 400
- Esin A., Narayan R., Ostriker E., Yi I., 1996, *ApJ*, 465, 312 (E96)
- Esin A., McClintock J. E. Narayan R., 1997, *ApJ*, 489, 865
- Fender R. P., Belloni T. M. Gallo, E., 2004, *MNRAS*, 355, 1105
- Gallo E., Fender R. P., Pooley G. G., 2003, *MNRAS*, 344, 60
- Gammie C. F., Popham R., 1998, *ApJ*, 498, 313
- Górecki A., Wilczewski W., 1984, *Acta Astr.*, 34, 141
- Grove J. E., Johnson W. N., Kroeger R. A., McNaron-Brown K., Skibo J. G., Philips B. F., 1998, *ApJ*, 500, 899
- Guilbert P. W., 1986, *MNRAS*, 218, 171
- Jaroszyński M., 2001, *Acta Astr.*, 51, 91
- Joinet A., Kalemci, E., Senziani, F., 2008, *ApJ*, 679, 655
- Kurpiewski A., Jaroszyński M., 1999, *A&A*, 346, 713
- Laurent P., Titarchuk L., 1999, *ApJ*, 511, 289
- Malzac J., Belmont R., 2009, *MNRAS*, 392, 570
- Manmoto T., Mineshige S., Kusunose M., 1997, *ApJ*, 489, 791
- Miller J. M., 2007, *ARA&A*, 45, 441
- Miller J. M., Homan J., Steeghs D., Rupen M., Hunstead R. W., Wijnands R., Charles P. A., Fabian A. C., 2006, *ApJ*, 653, 525
- Miyakawa T., Yamaoka K., Homan J., Saito K., Dotani T., Yoshida A., Inoue H., 2008, *PASJ*, 60, 637
- Narayan R., Yi I., 1994, *ApJ*, 428, L13
- Narayan R., Yi I., 1995, *ApJ*, 452, 710
- Narayan R., Mahadevan R. Quataert E., 1998, in *Theory of Black Hole Accretion Disks*, eds. M. A. Abramowicz, G. Björnsson, and J. E. Pringle. Cambridge University Press, p. 148
- Niedźwiecki A., 2005, *MNRAS*, 356, 913
- Niedźwiecki A., Zdziarski, A. A., 2006, *MNRAS*, 365, 606 (NZ06)
- Paczyński B., Wiita P. J., 1980, *A&A*, 88, 23
- Park M., Ostriker J. P., 1999, *ApJ*, 527, 247
- Park M., Ostriker J. P., 2001, *ApJ*, 549, 100
- Park M., Ostriker J. P., 2007, *ApJ*, 655, 88
- Poutanen J., Vurm I., 2009, *ApJ*, 690, L97
- Pozdnyakov L. A., Sobol' I. M., Sunyaev R. A., 1983, *Appl. Space Phys. Rev.*, 2, 189
- Quataert E., Gruzinov A., 1999, *ApJ*, 520, 248
- Quataert E., Narayan R., 1999, *ApJ*, 520, 298
- Shakura N. I., Sunyaev R. A., 1973, *A&A*, 24, 337
- Sharma, P., Quataert, E., Hammett, G. W., Stone, J. M., 2007, *ApJ*, 667, 714
- Stone, J. M., Pringle, J. E., Begelman, M. C., 1999, *MNRAS*, 310, 1002
- Sunyaev R. A., Titarchuk L. G., 1980, *A&A*, 86, 121
- Titarchuk L., Mastichiadis A., Kylafis N. D., 1997, *ApJ*, 487, 834
- Wardziński G., Zdziarski A. A., Gierliński M., Grove J. E., Jahoda K., Johnson W. N., 2002, *MNRAS*, 337, 829
- Yamaoka K., Miyakawa T. G., Saito K., Uzawa M., Arai M., Sakamoto H., Yamazaki T., Yoshida A., 2006, in *Proceedings VI Microquasar Workshop: Microquasars and Beyond*. Proc. Sci., SISSA, Trieste, p. 102
- Yuan F., 2001, *MNRAS*, 324, 119 (Y01)
- Yuan F., 2003, *ApJ*, 594, L99
- Yuan F., Zdziarski A. A., 2004, *MNRAS*, 354, 953
- Yuan F., Quataert E., Narayan R., 2003, *ApJ*, 598, 301
- Yuan F., Cui W., Narayan R., 2005, *ApJ*, 620, 905
- Yuan F., Shen Z. Q., Huang L., 2006, *ApJ*, 642, L45
- Yuan F., Zdziarski A. A., Xue Y., Wu X.-B., 2007, *ApJ*, 659, 541
- Yuan F., Xie F. G., Ostriker J. P., 2009, *ApJ*, 691, 98 (YX09)
- Zdziarski A. A., Gierliński M., 2004, *Progr. Theor. Phys. Suppl.*, 155, 99
- Zdziarski A. A., Poutanen J., Paciesas W. S., Wen L., 2002, *ApJ*, 578, 357
- Zdziarski A. A., Gierliński M., Mikolajewska J., Wardziński G., Smith D. M., Harmon B. A., Kitamoto S., 2004, *MNRAS*, 351, 791